Research Square

Preprints are preliminary reports that have not undergone peer review.
They should not be considered conclusive, used to inform clinical practice,
or referenced by the media as validated information.

Soil aggregate size modulates microbial metabolic regulation of soil carbon priming and sequestration in subalpine conifer and broadleaf forests

Chunxue Wei
Kaikui Chang
Chunyan Long
Xin Quan
Xiaoli Cheng
xlcheng@fudan.edu.cn

Yunnan University https://orcid.org/0000-0002-0346-675X

Research Article

Keywords: Priming effects, Net C sequestration, Soil aggregate size, Microbial metabolic strategies, Microbial carbon use efficiency

Posted Date: November 16th, 2026

DOI: https://doi.org/10.21203/rs.3.rs-11375085/v1

License: This work is licensed under a Creative Commons Attribution 4.0 International License.
Read Full License

Soil aggregate size modulates microbial metabolic regulation of soil carbon priming and sequestration in subalpine conifer and broadleaf forests

Chunxue Wei[1#], Kaikui Chang[3#], Chunyan Long[4], Xin Quan[1,2], Xiaoli Cheng[1, 2]*

[1] *State Key Laboratory of Vegetation Structure, Function and Construction (VegLab)*, *School of Ecology and Environmental Sciences, Yunnan University, Kunming 650091, P.R. China.*

[2] *Yunnan Key Laboratory of Soil Erosion Prevention and Green Development, Institute of International Rivers and Eco-security, Yunnan University, Kunming 650091, P.R. China.*

[3] *Bijie Ecological and Environmental Monitoring Center, Guizhou 551700, P.R. China*.

[4] *Research Center for Global Change and Ecological Forecasting, School of Ecological and Environmental Sciences, East China Normal University, Shanghai 200241, P.R. China.*

*Corresponding author: Dr. Xiaoli Cheng, Email: xlcheng@ynu.edu.cn

State Key Laboratory for Vegetation Structure, Functions and Construction (VegLab), Key Laboratory of Soil Ecology and Health in Universities of Yunnan Province, School of Ecology and Environmental Sciences, Yunnan University, Kunming 650091, PR China.

Phone: (86)-0871-65033547

[#] Joint first authors: These authors contributed equally to this work.

Abstract

Background and aims Fresh carbon and nutrient inputs influence soil organic carbon (SOC) dynamics through altering microbial C retention and native SOC decomposition. However, how these responses vary among soil aggregate fractions and relate to microbial metabolic processes remains unclear.

Methods We conducted an incubation with ^{13}C-labeled glucose and NH_4Cl using bulk soil and three aggregate fractions (1-2 mm, 0.25-1 mm, and <0.25 mm) from broad-leaved and coniferous forest soils. We quantified priming effects and short-term net C sequestration potential and examined their relationships with estimated microbial C use efficiency (CUE), the metabolic quotient (qCO_2), resource availability, and extracellular enzyme activities.

Results Despite contrasting initial soil properties between the two forest types, the overall magnitude of SOC priming effects did not differ significantly. Glucose addition induced positive priming effect regardless of N supply, while the effect of N addition on glucose-induced priming was weak or negative. Under glucose addition, priming effect declined and net C sequestration became less negative with decreasing aggregate size, despite higher SOC concentrations in smaller fractions. Estimated CUE was positively associated with net C sequestration, while qCO_2 generally decreased with decreasing aggregate size. PLS-PM and variance partitioning indicated that soil resource and microbial biomass variables were more prominent correlates of microbial C processing in larger aggregates, whereas enzyme-related associations were more evident in smaller fractions.

Conclusion These results identify soil aggregate size as an important context for interpreting short-term priming and C balance, with weaker priming in smaller fractions occurring alongside differences in resource availability and microbial metabolic indicators.

Keywords: Priming effects; Net C sequestration; Soil aggregate size; Microbial metabolic strategies; Microbial carbon use efficiency

Introduction

Forest soils store substantial amounts of terrestrial soil organic carbon (SOC), and the long-term persistence of SOC is jointly governed by plant-derived carbon (C) inputs and microbially mediated SOC turnover (Lehmann et al., 2020; Domeignoz-Horta et al., 2020; Tao et al., 2023). Labile C inputs from litter, roots, and rhizodeposition, provide substrates for microbial growth and SOC formation, but they can accelerate the decomposition of native SOC, trigger positive priming effects (PE) (Jones et al., 2009; Pausch and Kuzyakov 2018; Siles et al., 2022; Karhu et al., 2022). The strength of priming varies with soil resource availability and microbial nutrient limitation, particularly nitrogen (N) and phosphorus (P) availability (Bastida et al., 2019; Karhu et al., 2022; Ma et al., 2024). Microbial acquisition of labile C can intensify microbial nutrient demand, stimulating extracellular enzyme production and the decomposition of native soil organic matter (SOM) to acquire limiting nutrients (Karhu et al., 2022; Qi et al., 2024). In contrast, mineral nutrient supply alleviates nutrient-mining, thereby suppressing priming intensity under N-limited conditions (Feng and Zhu 2021). These contrasting microbial processes ultimately determine net soil C balance, which integrates newly fixed C retention and native SOC loss via priming (Liu et al., 2020; Karhu et al., 2022; Tao et al., 2023). Clarifying the regulatory mechanisms underlying such C balance is essential for understanding forest soil C sequestration under fluctuating resource availability.

Soil aggregates serve as fundamental physical and biotic habitats that reshape SOC stabilization and microbial metabolic processes (Six et al., 2004; Lehmann et al., 2020; Liu et al., 2021; Inagaki et al., 2023). Aggregation formation physically protects SOM by separating organic substrates from decomposers and extracellular enzymes, and hence promoting organo-

mineral associations (Six et al., 2002; Lehmann et al., 2020; Witzgall et al., 2021; Inagaki et al., 2023). The degree of this protection varies with aggregate size. Macroaggregates commonly contain relatively recent and accessible particulate organic matter, whereas microaggregates tend to retain older C through occlusion and mineral association (Witzgall et al., 2021; Georgiou et al., 2022; Inagaki et al., 2023). Isotope-labeling studies further reported that macroaggregates exhibit greater SOM derived CO_2 production and stronger glucose-induced priming than microaggregates (Tian et al., 2015, 2016; Husain et al., 2024). Beyond physical protection, aggregate size modulates microhabitat resource availability, shaping microbial biomass, community structure, and extracellular enzyme activities (Liu et al., 2021; Husain et al., 2024). These contrasting conditions may determine whether fresh C is preferentially retained through microbial growth or accompanied by greater losses of native SOC. Although the physical stabilization of SOC by soil aggregation is well documented (Lehmann et al. 2020; Witzgall et al., 2021; Georgiou et al., 2022), it remains poorly understood how aggregate size stratifies microbial regulatory pathways to modulate priming dynamics and net soil C sequestration.

Microbial metabolic traits, particularly carbon use efficiency (CUE) and metabolic quotient (qCO_2), provide a mechanistic link between aggregate microhabitats, resource availability, and soil C outcomes (Schimel and Schaeffer 2012). CUE quantifies the proportion of assimilated C allocated to growth rather than respiration (Geyer et al., 2016), with higher CUE facilitating microbial C retention, residue accumulation, and long-term SOC stabilization (Domeignoz-Horta et al., 2020; Tao et al., 2023; Cui et al., 2024). This mechanism is consistent well with the Microbial Efficiency-Matrix Stabilization framework, in which efficient microbial processing of labile substrates contributes substantially to stable SOC formation (Cotrufo et al., 2013; Kallenbach et al., 2016; Zhang Q et al., 2023). Conversely, qCO_2 are sensitive to substrate quality, nutrient stoichiometry, and enzyme allocation strategies (Spohn

et al., 2016; Domeignoz-Horta et al., 2020). Extracellular enzymes targeting C, N, and P further mediate resource acquisition across heterogeneous aggregate fractions, regulating microbial metabolic trade-offs between growth and respiration (Sinsabaugh et al., 2009; Moorhead et al., 2016; Karhu et al., 2022; Ma et al., 2024). Collectively, these complementary microbial metrics govern the balance between fresh C sequestration and native SOC priming. However, how their relative regulatory importance shifts with aggregate size remains unclear, limiting our mechanistic understanding of fraction-specific soil C dynamics.

Here, we investigated how soil aggregate size shapes microbial metabolic regulation of soil C priming and short-term net C sequestration potential in subalpine forest soils. Bulk soil and three aggregate fractions (1-2 mm, 0.25-1 mm, <0.25 mm) were collected from two typical subalpine forest types (*Pinus yunnanensis* coniferous forest and *Quercus pannosa* broadleaved forest) on Yulong Snow Mountain. A 29-day laboratory incubation experiment was conducted using ^{13}C-labeled glucose and NH_4Cl to simulate altered C and N availability, including control, single C addition, single N addition, and combined C and N addition treatments. By isotopically partitioning glucose-derived and native SOC-derived CO_2, we quantified aggregate-specific priming effects and net C sequestration potential, alongside key variables representing soil resource status, microbial biomass, metabolic traits (CUE and qCO_2), and extracellular enzyme activities. We tested two core hypotheses: (1) labile C addition would induce positive priming by stimulating microbial resource demand, while N addition would mitigate nutrient limitation and suppress priming to favor net C retention; (2) aggregate size would reshape SOC accessibility and microbial microenvironments, driving divergent patterns of priming and net C sequestration and differentiating the dominant regulatory pathways among soil resources, enzyme activities, and microbial metabolism. Overall, this study integrates aggregate-scale physical heterogeneity with microbial functional strategies, aiming

to advance a mechanistic framework for explaining context-dependent C priming and sequestration in forest soils.

Materials and methods

Study site and soil sampling

This study was conducted at Yulong Snow Mountain (27°0′04″-27°0′63″ N, 100°10′52″-100°11′02″ E; 3150-3250 m a.s.l), on the southeastern edge of the Qinghai-Tibet Plateau in the Hengduan Mountains (Men et al., 2025). The region has a subtropical South Asian monsoon climate, with a mean annual temperature of 12.7 °C and mean annual precipitation of 935 mm (Chen et al., 2022). A coniferous forest dominated by *Pinus yunnanensis* (*P. yunnanensis*) and a broad-leaved forest dominated by *Quercus pannosa* (*Q. pannosa*) were selected as contrasting forest types. According to the FAO taxonomy, both soils were classified as Luvisols, with sand, silt, and clay contents of 11%, 35%, and 45% in the coniferous forest soil, and 16%, 40%, and 44% in the broad-leaved forest soil, respectively (Liao et al., 2022).

One 30 × 30 m plot was established in each forest type. Within each plot, three 1 × 1 m subplots were randomly selected in areas with a relatively uniform distribution of the dominant tree species. After removing the litter layer, topsoil (0 -10 cm) was collected from multiple randomly selected locations within each plot and homogenized to form a composite sample. The soil samples were transported to the laboratory, passed through a 2 mm sieve, and visible fine-root fragments were removed. The unfractionated soil was retained as bulk soil, while a separate portion was used for aggregate fractionation.

Soil aggregate fractionation and incubation experiment

Soil aggregates were separated by wet sieving. Soil was passed sequentially through 2000-, 1000-, and 250-μm sieves to obtain three aggregate fractions (1-2 mm, 0.25-1 mm, and <0.25 mm). Each aggregate fraction was collected and divided into subsamples for subsequent

physicochemical, microbial, and incubation analyses.

Bulk soil and the three aggregate fractions from each forest soil were subjected to a 29-day laboratory incubation with exogenous C and N additions (Figure 1a). The experiment followed a factorial design with four soil fractions and four amendment treatments: control (deionized water), C addition (^{13}C-labeled glucose), N addition (NH_4Cl), and combined C plus N addition. Three replicate incubation units were established for each soil fraction × addition treatment combination, resulting in 48 incubation units for each forest soil.

For the incubation, 20 g of soil was placed in a 250 mL Erlenmeyer flask. Soil moisture was adjusted to 65% water-holding capacity with deionized water, and the soils were preincubated at 20 °C for 7 days before amendment. The amount of C added was equivalent to 100% of the microbial biomass C (MBC) of each soil fraction and was supplied as ^{13}C -labeled glucose. N was supplied as NH_4Cl at a substrate C: N ratio of 10, close to the ratio of dissolved organic C to mineral N used in the experimental design. Control and amendment solutions were added in a total volume of 2 ml. At the end of incubation, soil was collected for physicochemical, microbial, and extracellular enzyme analyses.

Soil physicochemical and microbial analyses

Soil properties were measured in bulk soil and all aggregate fractions. Soil pH was measured at a soil: water ratio of 1: 2.5. Soil C and N contents were measured using an elemental analyzer after removal of inorganic C (Flash 2000, Thermo Fisher Scientific, USA), and $\delta^{13}C$ was measured using an isotope-ratio mass spectrometer (Delta V Advantage, Thermo Fisher Scientific, Germany). Soil available N, defined as NH_4^+-N plus NO_3^--N, was extracted with 1 mol L^{-1} KCl and measured using a SmartChem discrete analyzer (Advanced Micro Systems Inc). Total P was determined after H_2SO_4/ $HClO_4$ digestion, and available P was measured using the hydrochloric acid–ammonium fluoride method.

Microbial biomass C and N were determined by chloroform fumigation-K_2SO_4 extraction.

After 24 h of fumigation, fumigated and unfumigated soils were extracted, and extractable organic C and N were measured using a TOC analyzer (Vario TO, Elementar). MBC and MBN were calculated using extraction coefficients of 0.45 and 0.54, respectively:

$$MBC = \frac{\Delta E_C}{K_C} \quad (1)$$

$$MBN = \frac{\Delta E_N}{K_N} \quad (2)$$

where ΔE_C is the difference in EOC between the fumigated and unfumigated soils; K_C is the extraction coefficient of MBC (0.45); ΔE_N is the difference in EON between the fumigated and unfumigated soils; K_N is the extraction coefficient of MBN (0.54).

Five extracellular enzymes involved in C, N, and P acquisition were measured: *α*-glucosidase (AG), *β*-1,4-glucosidase (BG), leucine aminopeptidase (LAP), *β*-1,4-N-acetylglucosaminidase (NAG), and alkaline phosphatase (AP). Enzyme assays were conducted in 96-well microplates and quantified spectrophotometrically at 450 nm (Thermo Fisher Scientific, Waltham, MA, USA).

Soil CO_2 efflux and $\delta^{13}C$ were measured at the end of the incubation. Headspace CO_2 was first removed by flushing the flasks with CO_2-free air, after which the flasks were sealed for a defined accumulation period. A 30-mL gas sample was collected from each flask and analyzed using an isotope analyzer (Picarro G2210-i, USA).

Calculations

CO_2 derived from native SOC and added glucose-C during incubation was partitioned using $\delta^{13}C$ as follows:

$$C_{\mathrm{SOC}} = C_{\mathrm{total}} \times \frac{\delta^{13}C_{\mathrm{total}} - \delta^{13}C_{\mathrm{Glu}}}{\delta^{13}C_{\mathrm{control}} - \delta^{13}C_{\mathrm{Glu}}} \quad (3)$$

$$C_{\mathrm{Glu/GluN}} = C_{\mathrm{total}} - C_{\mathrm{SOC}} \quad (4)$$

where C_{SOC} is the CO_2-C derived from native SOC and C_{total} is total CO_2-C released under the glucose or glucose plus N treatment. $C_{Glu/GluN}$ is CO_2-C derived from the added glucose

192 substrate. $\delta^{13}C$ total and $\delta^{13}C$control are the isotopic signatures of total CO_2 released from the
193 amended and control soils, respectively, and $\delta^{13}C$-Glu is the isotopic signature of the added
194 glucose-C.

195 The priming effect induced by glucose addition (PE_{Glu}) was calculated as the difference
196 in native SOC derived CO_2-C between the glucose treatment and the control. The priming
197 effect under combined glucose plus N addition (PE_{GluN}) was calculated relative to the N-only
198 treatment. The N-induced priming effect (PE_N) was calculated as the difference between
199 PE_{GluN} and PE_{Glu} following the approach reported previously (Feng et al.,2021). The
200 calculations were as follows:

201 $$PE_{\mathrm{Glu}}\ (\mathrm{mg\,C\,g^{-1}\,SOC}) = \frac{C_{\mathrm{Glu}} - C_{\mathrm{control}}}{SOC} \quad (5)$$

202 $$PE_{\mathrm{GluN}}\ (\mathrm{mg\,C\,g^{-1}\,SOC}) = \frac{C_{\mathrm{GluN}} - C_{\mathrm{control}}}{SOC} \quad (6)$$

203 $$PE_{N}\ (\mathrm{mg\,C\,g^{-1}\,SOC}) = PE_{\mathrm{GluN}} - PE_{\mathrm{Glu}} \quad (7)$$

204 where PE_{Glu}, PE_{GluN}, and PE_N denote priming effects associated with glucose, glucose plus N,
205 and N treatments, respectively; $C_{control}$, C_{Glu}, and C_{GluN} denote the corresponding native SOC-
206 derived CO_2-C terms used in the calculations.

207 Short-term net C sequestration potential was calculated from the balance between
208 retained added C and C lost as CO_2. The net C sequestration potential was expressed per unit
209 of added glucose-C as follows:

210 $$\text{Net C sequestration}\ (\%) = \frac{C_{\mathrm{retained}} - C_{\mathrm{Glu/GluN}}}{C_{\mathrm{addition}}} \times 100 \quad (8)$$

211 where $C_{retained}$ is the amount of added glucose-C retained in soil under glucose or glucose plus
212 N addition, $C_{Glu/GluN}$ is glucose-derived CO_2-C, and $C_{addition}$ is the amount of added glucose-C.
213 The N-only value was calculated from the difference between the combined glucose plus N
214 and glucose-only treatments. Because this metric represents a 29-day incubation balance, it is
215 interpreted here as short-term net C sequestration potential rather than direct evidence of long-

term SOC stabilization.

Microbial carbon use efficiency (CUE) was calculated using the geochemical equilibrium model:

$$CUE = CUE_{\max} \times \left(\frac{S_{C:N} \times S_{C:P}}{(K_{C:N}+S_{C:N}) \times (K_{C:P}+S_{C:P})}\right)^{0.5} \quad (9)$$

$$S_{C:N} = \frac{M_{C:N}}{L_{C:N}} \times \frac{1}{EEA_{C:N}} \quad (10)$$

$$S_{C:P} = \frac{M_{C:P}}{L_{C:P}} \times EEA_{C:P} \quad (11)$$

where $K_{C:N}$ and $K_{C:P}$ are half-saturation constants for CUE based on C, N and P availability, and were set at 0.50. CUE_{max} was set at 0.6. $S_{C:N}$ and $S_{C:P}$ represent the scalars of resource availability for microbial growth based on the stoichiometries of extracellular enzyme activities and SOM (Cui et al. 2020; Zhang D et al. 2023). $L_{C:N}$ and $L_{C:P}$ represent the C: X ratios of labile substrates. Labile C, N and P were DOC, inorganic N (the sum of $NH4^+$ and $NO3^-$) and available P, respectively. $M_{C:N}$ and $M_{C:P}$ are the ratios of MBC to MBN and MBC to MBP, respectively.

The microbial qCO_2 was calculated as CO_2-C released per unit of MBC on day 29:

$$qCO_2 = \frac{M_{CO_2}}{MBC} \quad (12)$$

where M_{CO_2} is microbial respiration-derived C and MBC is microbial biomass C measured at the end of incubation.

Statistical analysis

Statistical analyses were performed using R version 4.1.2. Normality and homogeneity of variance were assessed where required for parametric analyses. Within each forest soil, one-way analysis of variance (ANOVA) was used to assess differences among bulk soil and the three aggregate-size fractions. Response ratios (RR) were calculated as the ratio of each amendment treatment to its corresponding control. The effects of forest type, soil fractions, addition treatment, and their interactions on the PE and net C sequestration were evaluated

using multifactorial analysis. Linear regression was used to examine the relationships of net C sequestration with PE and CUE, with net C sequestration as the response variable and PE or CUE as the explanatory variable in separate models. Spearman correlation analysis was used to assess the direction and strength of associations among C-cycle responses, soil properties, microbial traits, and extracellular enzyme activities. Correlation matrices were visualized using the *corrplot* package in R. Variation partitioning analysis (VPA) was performed using the *vegan* package in R to quantify the unique and shared contributions of soil properties, microbial traits, and enzyme activities to variation in net C sequestration.

Partial least squares path modelling (PLS-PM) was used to examine potential pathways linking soil properties, microbial traits, and extracellular enzyme activities with CUE, qCO_2, PE, and net C sequestration across soil fractions. This model was constructed using the *plspm* package. We used bootstrap resamples to assess the uncertainty of path coefficients and coefficients of determination (R^2). The R^2 values indicated the proportion of variance explained in each endogenous variable. The goodness-of-fit (GoF) index was reported as a descriptive measure of overall model performance. Path coefficients indicated the direction and strength of relationships between variables. Indirect effects were calculated by multiplying the path coefficients along each specified pathway. The analysis assessed the relationships represented by the specified path structure and their relevance to microbial C processing and soil C balance. Path coefficients described the direction and strength of the modelled relationships, which were interpreted as associations consistent with the proposed pathways.

Results

Initial soil properties and microbial traits across forest soils and aggregate sizes

Initial soil properties differed significantly between the broad-leaved and coniferous forest soils (Fig. 1b; Fig. S1). Specifically, SOC, TN, DON and AP were significantly higher in the

coniferous forest soil than in the broad-leaved forest soil, while DOC and SOC: TN ratio were significantly lower in the coniferous forest. Across soil aggregate sizes, SOC, TN, DOC, and DON increased with decreasing aggregate size in both coniferous and broad-leaved forest soils, with the highest concentrations occurring in the <0.25 mm aggregates. The SOC:TN ratio and AP were significantly lower in the <0.25 mm aggregates than in the other soil fractions in both forest soils (Fig. 1b). Initial soil pH and NH_4^+-N concentrations were higher in the coniferous forest soil, whereas NO_3^--N concentrations were higher in the broad-leaved forest soil across the soil fractions (Fig. S1). Litter C concentrations and C: N ratios were higher in the coniferous forest than in the broad-leaved forest, whereas litter N concentrations were lower (Table S1).

As for microbial attributes, MBC and MBN were significantly higher in the coniferous forest soil than in the broad-leaved forest soil across bulk soil and all aggregate fractions (Fig. 2a, b). Within each forest soil, MBC and MBN increased with decreasing aggregate size and were positively correlated with each other (Fig 2c). C- and N-acquiring enzyme activities were generally higher in smaller aggregates than in the 1-2 mm aggregate fractions in both forest soils (Fig. 2d; Fig. S2a, b). In contrast, P-acquiring enzyme activity showed different patterns between the two forest soils, with relatively high activity in bulk broad-leaved forest soil and in the <0.25 mm aggregates of coniferous forest soil (Fig. 2d; Fig. S2c). Enzyme stoichiometric patterns were similar between the two forest soils, with overlapping distributions of enzyme activity ratios (Fig. 2e). All observations lay above the 1:1 line, indicating that the ratio of C- to combined C- and N-acquiring enzyme activities exceeded the corresponding ratio for C- and P-acquiring activities. Enzyme vector length did not differ significantly between forest soils or among soil fractions, whereas vector angles exceeded 45° in all groups (Fig. 2f).

Soil aggregate-size-dependent responses of C priming and net C sequestration to C and N

addition

PE was not significantly different between broad-leaved and coniferous forest soils, while C and N additions and soil aggregate sizes strongly affected priming effects (Table S2). The direction and magnitude of PE differed markedly among C and N addition treatments. C and C plus N addition induced positive PE across all soil fractions, while N addition resulted in weak or negative priming effects in both forest soils (Fig. 3a, b). The PE also varied strongly among soil fractions, with the highest values occurring in the 1-2 mm aggregates followed by 0.25-1 mm and <0.25 mm aggregates.

Net C sequestration was affected by forest type, C and N additions, and soil aggregates (Table S2). In contrast to N addition, C and C plus N addition caused net soil C loss in both forest soils, whereas N addition promoted net soil C accumulation (Fig. 3c, d). The magnitude of these responses was also dependent on aggregate size. Under C and C plus N addition, Net C sequestration increased with decreasing aggregate size, whereas N addition showed the opposite trend across the <2 mm soil aggregate fractions (Fig. 3c, d). Thus, C and N additions produced contrasting effects on native C priming and net C sequestration, with these responses varying systematically among aggregate fractions.

Soil aggregate size and nutrient addition shape microbial metabolic strategies

CUE was significantly higher in the coniferous forest soil than in the broad-leaved forest soil, whereas the microbial metabolic quotient (qCO_2) was significantly lower in the coniferous forest soil ($P < 0.05$). CUE and qCO_2 were significantly higher under N addition than under C and C plus N addition (Fig. 4) in both forest soils. CUE was significantly higher in larger soil aggregates except under C addition (Fig. 4a, b). qCO_2 significantly decreased with decreasing aggregate size under all amendment treatments (Fig. 4c, d). In addition, there were no significant differences in the response ratios of CUE and qCO_2 between the two forest soils. The response ratio of CUE in 1-2 mm soil aggregates increased significantly under all addition

315 treatments (Fig. S3a, b). The response ratio of qCO_2 in 1-2 mm soil aggregates decreased
316 significantly under all amendment treatments (Fig. S3c, d).

317 ***Microbial carbon use efficiency and priming regulate net C sequestration***

318 The aggregate size dependent responses of net C sequestration were closely associated with
319 microbial C-processing characteristics. Across forest types, C and N additions, and aggregate
320 fractions, priming effects were negatively correlated with net C sequestration, whereas CUE
321 was positively associated with net C sequestration (Fig. 5a, b).

322 The relationships among soil properties, microbial traits, enzyme activities, and microbial
323 metabolic strategies revealed distinct aggregate-size-dependent patterns (Fig. 5c, d). DOC and
324 DON increased with decreasing aggregate size across C and N addition treatments, while AN
325 and AP generally decreased with decreasing aggregate size (Fig. S5). MBC, MBC: MBN ratio,
326 and enzyme activities, including C-acquiring and P-acquiring enzymes, also increased with
327 decreasing aggregate size (Fig. S6).

328 C and N additions modified these aggregate-specific responses. Compared with the
329 control, DOC, DON, and AN were significantly increased in 1-2 mm aggregates, whereas AP
330 was reduced under all addition treatments (Fig. S5). Similarly, MBC, MBC: MBN ratio, and
331 enzyme activities were significantly increased in 1-2mm aggregates following C and N
332 additions (Fig. S6).

333 ***Soil aggregate size alters the pathways linking soil properties, microbial traits and C***
334 ***sequestration***

335 The PLS-PM identified soil aggregate size dependent pathways linking soil properties,
336 microbial traits, microbial metabolic strategies and C sequestration. In bulk soil, soil properties
337 and microbial traits were positively associated with CUE, whereas enzyme activity was
338 negatively correlated with qCO_2 (Fig. 6a). The relative importance of these pathways changed
339 with aggregate size. In 1-2 mm soil aggregates, soil properties and microbial traits were the

main factors associated with lower PE through higher CUE and lower qCO_2 (Fig. 6c). In smaller soil aggregates, enzyme activity became a more prominent factor associated with microbial metabolism. Enzyme activity showed negative associations with qCO_2, while enhanced microbial respiration was associated with greater C loss (Fig. 6c, d).

Discussion

Resource availability modulates glucose-induced SOC priming

Glucose addition induced positive priming effects in both forest soils, indicating that fresh C inputs stimulated the mineralization of native SOC (Fig. 3). This response is consistent with the proposed coupling between labile C supply and microbial nutrient acquisition (Bastida et al., 2019; Karhu et al., 2022). Readily available C can support microbial activity while increasing nutrient requirements for growth. When inherent soil nutrient pools cannot satisfy microbial growth requirements, microorganisms adopt a nutrient-mining strategy by decomposing recalcitrant native SOM, thereby increasing SOC-derived CO_2 release (Feng and Zhu 2021; Ma et al., 2024). Accordingly, nutrient mining provides a plausible explanation for the observed positive priming effect.

The addition of mineral N exerted weak or negative effects on glucose-induced priming, indicating that exogenous N supply did not amplify, but instead partially mitigated, fresh C-triggered native SOC decomposition. This pattern suggests that mineral N supply reduces microbial dependence on SOM-derived nutrients and alleviates nutrient mining pressure (Feng and Zhu 2021; Qi et al., 2024). Nevertheless, combined C and N addition still generated significant positive priming effect, indicating that N enrichment cannot fully offset or eliminate C-induced priming responses. Collectively, these results imply that priming magnitude is modulated by the stoichiometric balance between substrate supply and microbial nutrient requirements, rather than being solely controlled by N limitation (Karhu et al., 2022;

Ma et al., 2024).

Despite contrasting initial soil properties between coniferous and broadleaved forests, bulk soil priming effect did not differ significantly between the two forests. This similarity indicates that short-term priming responses to pulsed labile C inputs are relatively convergent across these two subalpine forest soils, although forest type effects may emerge over longer temporal scales or under chronic substrate input regimes. The net soil C balance ultimately depends on the trade-off between newly added C retention and priming-mediated native SOC loss, which is highly sensitive to resource input conditions rather than static forest soil properties.

Aggregate-size-dependent priming intensity and short-term C balance

Soil aggregate fractions exhibited divergent priming responses to C and N inputs, revealing a clear size-dependent pattern: priming effects gradually declined with decreasing aggregate size across both forest soils. Specifically, the 1-2 mm macroaggregates showed the strongest positive priming, while the 0.25-1 mm and <0.25 mm microaggregates displayed progressively attenuated priming intensity (Fig. 3a, b). The gradual decline in priming effect with decreasing aggregate size is consistent with our hypothesis that stronger physical protection in smaller aggregates restricts microbial access to native SOC and reduces priming-induced SOC decomposition. Soil aggregate size heterogeneity fundamentally reshapes substrate availability and microhabitat conditions for soil microorganisms (Dungait et al., 2012; Lehmann et al., 2020; Witzgall et al., 2021; Liu et al., 2021). Macroaggregates generally contain more spatially accessible and relatively weakly protected organic matter. Following labile C input, enhanced microbial activity and extracellular enzyme production rapidly decompose unprotected native SOM, generating intensive priming in large aggregates (Tian et al., 2015, 2016; Liu et al., 2021; Husain et al., 2024). In contrast, SOM within microaggregates is largely stabilized through tight physical occlusion and organo-mineral

association, which spatially decouples organic substrates from microbial decomposers and extracellular enzymes (von Lützow et al., 2006; Kögel-Knabner et al., 2008). This physical isolation persists even under elevated labile C availability, effectively suppressing priming decomposition in fine aggregate fractions.

Notably, SOC and nutrient concentrations increased progressively with decreasing aggregate size, forming a striking contrast with the declining priming intensity across fractions (Fig. 3). This inconsistency demonstrates that SOC stock size does not equate to microbial decomposability, and FSOC accessibility rather than quantity dominates priming regulation (Schmidt et al., 2011; Inagaki et al., 2023). Such evidence reinforces the modern framework of SOC stabilization, in which aggregate-mediated physical protection constrains substrate bioavailability and governs SOC persistence (Lehmann and Kleber 2015). Importantly, the concurrent variation in CUE and qCO_2 across soil aggregates (Fig. 4) further suggests that microbially mediated metabolic regulation acts as a complementary mechanism, alongside physical protection, to modulate fraction-specific C priming and net sequestration.

Microbial metabolic regulation and fraction-specific C sequestration mechanisms

Microbial metabolic traits directly shape the short-term soil C balance by regulating the partitioning of assimilated C toward either growth retention or respiratory loss. Our study revealed consistent positive correlations between net C sequestration and CUE, alongside negative associations between net C sequestration and priming intensity (Fig. 5). Higher CUE facilitates greater C allocation to microbial biomass production and necromass accumulation, which constitutes a key pathway for stable SOC formation (Kallenbach et al., 2016; Zhang Q et al., 2023; Tao et al., 2023). However, fraction-specific variations in priming and net C balance cannot be fully explained by CUE alone. The 1-2mm macroaggregates exhibited the strongest priming and the most negative net C balance under glucose addition, yet they did not show consistently lower CUE relative to microaggregates. Instead, macroaggregates harbored

significantly higher qCO_2 , indicating a higher respiratory cost relative to microbial biomass. This interpretation confirms that net soil C balance is determined by the trade-off between microbial C retention and respiratory decomposition, rather than by only CUE (Manzoni et al., 2012; Sinsabaugh et al., 2013). Even when labile C promotes efficient microbial growth and biomass accumulation, intensified priming decomposition and high respiratory costs in macroaggregates can completely offset newly retained C, resulting in net soil C loss (Kuzyakov 2010; Kallenbach et al., 2016; Tao et al., 2023).

Aggregate-scale resource stoichiometry and enzyme allocation further reshape microbial metabolic strategies. Decreasing aggregate size corresponded to elevated dissolved C and nutrient heterogeneity, combined with divergent microbial biomass parameters and extracellular enzyme activities (Figs S5, S6). Variable resource availability across fractions drives distinct microbial investment trade-offs between growth maintenance and resource acquisition (Burns et al., 2013; Karhu et al., 2022; Cui et al., 2024). Microorganisms in resource-open macroaggregates tend to prioritize rapid growth and SOM mining, whereas those in protected microaggregates adopt metabolically conservative strategies with lower respiratory consumption and reduced enzyme investment in native SOM decomposition. PLS-PM and variance partitioning explicitly demonstrated a systematic shift in dominant regulatory pathways across aggregate fractions (Fig. 6; Fig. S4). In bulk soil and macroaggregates (1-2 mm), soil physicochemical properties and microbial biomass traits were the primary drivers of microbial metabolism and priming variation. In contrast, extracellular enzyme activities exerted increasingly dominant control on microbial C processing as aggregate size decreased, with enzyme variables explaining the largest unique proportion of variance in microaggregates (<0.25 mm). This structural shift highlights a core regulatory paradigm: SOC turnover in large aggregates is primarily constrained by resource availability and microbial biomass, whereas microaggregate C dynamics depend heavily on enzyme-mediated substrate acquisition under

strong physical isolation (Kleber et al., 2007; Witzgall et al., 2021; Inagaki et al., 2023; Husain et al., 2024).

Conclusion and implications

This study systematically demonstrates that soil aggregate size mediates short-term SOC priming and net C sequestration through the integrated regulation of physical protection and microbial metabolic strategies under variable C and N availability. Labile C addition insistently induced positive priming and reduced net C sequestration potential, while N addition alleviated nutrient mining and mitigated priming intensity, favoring soil C retention. Priming intensity declined monotonically with decreasing aggregate size, corresponding to stronger physical protection of native SOC in microaggregates. The trade-off between microbial C retention (quantified as CUE) and priming-induced SOC decomposition fundamentally determines the short-term net soil C balance. The shifts in regulatory pathways further suggest that soil resource and microbial biomass dominate C cycling in macroaggregates, whereas enzyme-mediated microbial regulation prevails in microaggregates. By integrating aggregate-dependent physical stabilization and microbial metabolic mechanisms, this study provides a refined microscale framework for understanding heterogeneous SOC responses to changing resource availability in subalpine forest soils, highlighting the necessity of resolving aggregate-scale processes for accurate forest soil C cycle prediction.

It should be noted that this study is based on a short-term (29-day) incubation experiment with pulsed labile C addition. Short-term priming responses and microbial metabolic trade-offs may differ from long-term SOC stabilization processes driven by microbial necromass accumulation and mineral-associated SOC formation (Lavallee et al., 2020; Tao et al., 2023). Future fraction-resolved C tracing studies with extended incubation durations are required to

validate the persistence of aggregate-scale microbial metabolic regulation under chronic resource inputs.

Acknowledgements

This research was financially supported by the National Key R&D Program of China (2024YFF1306700) and the Yunnan Fundamental Research Projects (202601BC070004). We are grateful to Lijiang Forest Biodiversity National Observation and Research Station for help with fieldwork.

Author contributions

Chunxue Wei: data curation, formal analysis, writing - original draft. **Kaikui Chang:** data curation, visualization, writing - original draft. **Chunyan Long:** methodology. **Xin Quan:** investigation. **Xiaoli Cheng:** conceptualization, methodology, funding acquisition, writing - review and editing.

Conflict of interest statement

The authors declare that they do not have any commercial or associative interest that represents a conflict of interest.

Data availability

We agree to archive the data associated with this manuscFript should the manuscript be accepted.

Reference

FBastida F, García C, Fierer N, Eldridge DJ, Bowker MA, Abades S, Alfaro FD, Berhe AA, Cutler NA, Gallardo A, García-Velázquez L, Hart SC, Hayes PE, Hernández T, Hseu ZY, Jehmlich N, Kirchmair M, Lambers H, Neuhauser S, Peña-Ramírez VM, Pérez CA, Reed SC, Santos F, Siebe C, Sullivan BW, Trivedi P, Vera A, Williams MA, Moreno JL, Delgado-Baquerizo M (2019) Global ecological predictors of the soil priming effect. Nat Commun 10 (1):3481. https://doi.org/10.1038/s41467-019-11472-7

Burns RG, DeForest JL, Marxsen J, Sinsabaugh RL, Stromberger ME, Wallenstein MD, Weintraub MN, Zoppini A (2013) Soil enzymes in a changing environment: current knowledge and future directions. Soil Biol Biochem 58:216–234. https://doi.org/10.1016/j.soilbio.2012.11.009

Chen Q, Chen J, Andersen MN, Cheng X (2022) Elevational shifts in foliar-soil $\delta^{15}N$ in the Hengduan Mountains and different potential mechanisms. Glob Change Biol 28 (18):5480–5491. https://doi.org/10.1111/gcb.16306

Cotrufo MF, Wallenstein MD, Boot CM, Denef K, Paul E (2013) The Microbial Efficiency-Matrix Stabilization (MEMS) framework integrates plant litter decomposition with soil organic matter stabilization: do labile plant inputs form stable soil organic matter? Glob Change Biol 19 (4):988–995. https://doi.org/10.1111/gcb.12113

Cui Y, Hu J, Peng S, Delgado-Baquerizo M, Moorhead DL, Sinsabaugh RL, Xu X, Geyer KM, Fang L, Smith P, Peñuelas J, Kuzyakov Y, Chen J (2024) Limiting resources define the global pattern of soil microbial carbon use efficiency. Adv Sci 11 (35):2308176. https://doi.org/10.1002/advs.202308176

Cui Y, Wang X, Zhang X, Ju W, Duan C, Guo X, Wang Y, Fang L (2020) Soil moisture mediates microbial carbon and phosphorus metabolism during vegetation succession in a semiarid region. Soil Biol Biochem 147:107814. https://doi.org/10.1016/j.soilbio.2020.107814

Domeignoz-Horta LA, Pold G, Liu XJA, Frey SD, McMahon JM, DeAngelis KM (2020) Microbial diversity drives carbon use efficiency in a model soil. Nat Commun 11 (1):3684. https://doi.org/10.1038/s41467-020-17502-z

Dungait JAJ, Hopkins DW, Gregory AS, Whitmore AP (2012) Soil organic matter turnover is governed by accessibility not recalcitrance. Glob Change Biol 18 (6):1781–1796. https://doi.org/10.1111/j.1365-2486.2012.02665.x

Feng J, Tang M, Zhu B (2021) Soil priming effect and its responses to nutrient addition along a tropical forest elevation gradient. Glob Change Biol 27 (12):2793–2806. https://doi.org/10.1111/gcb.15587

Feng J, Zhu B (2021) Global patterns and associated drivers of priming effect in response to nutrient addition. Soil Biol Biochem 153:108118. https://doi.org/10.1016/j.soilbio.2020.108118

Georgiou K, Jackson RB, Vindušková O, Abramoff RZ, Ahlström A, Feng W, Harden JW, Pellegrini AFA, Polley HW, Soong JL, Riley WJ, Torn MS (2022) Global stocks and capacity of mineral-associated soil organic carbon. Nat Commun 13 (1):3797. https://doi.org/10.1038/s41467-022-31540-9

Geyer KM, Kyker-Snowman E, Grandy AS, Frey SD (2016) Microbial carbon use efficiency: accounting for population, community, and ecosystem-scale controls over the fate of metabolized organic matter. Biogeochemistry 127:173–188. https://doi.org/10.1007/s10533-016-0191-y

Husain H, Keitel C, Dijkstra FA (2024) Fungi are more important than bacteria for soil carbon loss through priming effects and carbon protection through aggregation. Appl Soil Ecol 195:105245. https://doi.org/10.1016/j.apsoil.2023.105245

Inagaki TM, Possinger AR, Schweizer SA, Mueller CW, Hoeschen C, Zachman MJ, Kourkoutis LF, Kögel-Knabner I, Lehmann J (2023) Microscale spatial distribution and soil organic matter persistence in top and subsoil. Soil Biol Biochem 178:108921. https://doi.org/10.1016/j.soilbio.2022.108921

Jones DL, Nguyen C, Finlay RD (2009) Carbon flow in the rhizosphere: carbon trading at the soil-root interface. Plant Soil 321 (1-2):5–33. https://doi.org/10.1007/s11104-009-9925-0

Kallenbach CM, Frey SD, Grandy AS (2016) Direct evidence for microbial-derived soil organic matter formation and its ecophysiological controls. Nat Commun 7 (1):13630. https://doi.org/10.1038/ncomms13630

Karhu K, Alaei S, Li J, Merilä P, Ostonen I, Bengtson P (2022) Microbial carbon use efficiency and priming of soil organic matter mineralization by glucose additions in boreal forest soils with different C: N ratios. Soil Biol Biochem 167:108615. https://doi.org/10.1016/j.soilbio.2022.108615

Kleber M, Sollins P, Sutton R (2007) A conceptual model of organo-mineral interactions in soils: self- assembly of organic molecular fragments into zonal structures on mineral surfaces. *Biogeochemistry* 85:9–24. https://doi.org/10.1007/s10533-007-9103-5

Kuzyakov Y (2010) Priming effects: interactions between living and dead organic matter. Soil Biol Biochem 42:1363–1371. https://doi.org/10.1016/j.soilbio.2010.04.003

Kögel-Knabner I, Guggenberger G, Kleber M, Kandeler E, Kalbitz K, Scheu S, Eusterhues K, Leinweber P (2008) Organo- mineral associations in temperate soils: integrating biology, mineralogy, and organic matter chemistry. J Plant Nutr Soil Sci 171 (1):61–82. https://doi.org/10.1002/jpln.200700048

Lavallee JM, Soong JL, Cotrufo MF (2020) Conceptualizing soil organic matter into particulate and mineral-associated forms to address global change in the 21st century. Glob Change Biol 26 (1):261–273. https://doi.org/10.1111/gcb.14859

Lehmann J, Hansel CM, Kaiser C, Kleber M, Maher K, Manzoni S, Nunan N, Reichstein M, Schimel JP, Torn MS, Wieder WR, Kögel-Knabner I (2020) Persistence of soil organic carbon caused by functional complexity. Nature Geoscience 13 (8):529–534. https://doi.org/10.1038/s41561-020-0612-3

Lehmann J, Kleber M (2015) The contentious nature of soil organic matter. Nature 528 (7580):60–68. https://doi.org/10.1038/nature16069

Liao C, Men X, Wang C, Chen R, Cheng X (2022) Nitrogen availability and mineral particles contributed fungal necromass to the newly formed stable carbon pool in the alpine areas of Southwest China. Soil Biol Biochem 173:108788. https://doi.org/10.1016/j.soilbio.2022.108788

Liu XJA, Finley BK, Mau RL, Schwartz E, Dijkstra P, Bowker MA, Hungate BA (2020) The soil priming effect: Consistent across ecosystems, elusive mechanisms. Soil Biol Biochem 140:107617. https://doi.org/10.1016/j.soilbio.2019.107617

Liu XJA, Pold G, Domeignoz-Horta LA, Geyer KM, DeAngelis KM (2021) Soil aggregate-mediated microbial responses to long-term warming. Soil Biol Biochem 152:108055. https://doi.org/10.1016/j.soilbio.2020.108055

Ma T, Zhan Y, Chen W, Hou Z, Chai S, Zhang J, Zhang X, Wang R, Liu R, Wei Y (2024) Microbial traits drive soil priming effect in response to nitrogen addition along an alpine forest elevation gradient. Sci Total Environ 907:167970. https://doi.org/10.1016/j.scitotenv.2023.167970

Manzoni S, Taylor P, Richter A, Porporato A, Ågren GI (2012) Environmental and stoichiometric controls on microbial carbon-use efficiency in soils. New Phytol 196:79–91. https://doi.org/10.1111/j.1469-8137.2012.04225.x

Men X, Bao Y, Zhai D, Huang B, Quan X, He X, Yang H, Cheng X (2025) Soil microbial

metabolic limitations under subalpine coniferous and broad-leaved forests responding to litter input and removal treatments. Funct Ecol 39:2803–2816. https://doi.org/10.1111/1365-2435.70136
Moorhead DL, Sinsabaugh RL, Hill BH, Weintraub MN (2016) Vector analysis of eco-enzyme activities reveal constraints on coupled C, N and P dynamics. Soil Biol Biochem 93:1–7. https://doi.org/10.1016/j.soilbio.2015.10.019
Pausch J, Kuzyakov Y (2018) Carbon input by roots into the soil: quantification of rhizodeposition from root to ecosystem scale. Glob Change Biol 24 (1):1–12. https://doi.org/10.1111/gcb.13850
Qi D, Huang G, Feng Y, He X, Song Y, Song F (2024) Nitrogen addition suppresses soil positive priming effect in temperate plantations: Evidence from an 8-year in situ field experiment. Funct Ecol 38 (2):429–438. https://doi.org/10.1111/1365-2435.14484
Schimel JP, Schaeffer SM (2012) Microbial control over carbon cycling in soil. Front Microbiol 3:348. https://doi.org/10.3389/fmicb.2012.00348
Schmidt MWI, Torn MS, Abiven S, Dittmar T, Guggenberger G, Janssens IA, Kleber M, Kögel-Knabner I, Lehmann J, Manning DAC, Nannipieri P, Rasse DP, Weiner S, Trumbore SE (2011) Persistence of soil organic matter as an ecosystem property. Nature 478 (7367):49–56. https://doi.org/10.1038/nature10386
Siles JA, Díaz-López M, Vera A, Eisenhauer N, Guerra CA, Smith LC, Buscot F, Reitz T, Breitkreuz C, Van den Hoogen J, Crowther TW, Orgiazzi A, Kuzyakov Y, Delgado-Baquerizo M, Bastida F (2022) Priming effects in soils across Europe. Glob Change Biol 28 (6):2146–2157. https://doi.org/10.1111/gcb.16062
Sinsabaugh RL, Hill BH, Follstad Shah JJ (2009) Ecoenzymatic stoichiometry of microbial organic nutrient acquisition in soil and sediment. *Nature* 462:795–798. https://doi.org/10.1038/nature08632
Sinsabaugh RL, Manzoni S, Moorhead DL, Richter A (2013) Carbon use efficiency of microbial communities: stoichiometry, methodology and modelling. Ecol Lett 16 (7):930–939. https://doi.org/10.1111/ele.12113
Six J, Bossuyt H, Degryze S, Denef K (2004) A history of research on the link between (micro)aggregates, soil biota, and soil organic matter dynamics. Soil Tillage Res 79:7–31. https://doi.org/10.1016/j.still.2004.03.008
Six J, Conant RT, Paul EA, Paustian K (2002) Stabilization mechanisms of soil organic matter: implications for C-saturation of soils. Plant Soil 241:155–176. https://doi.org/10.1023/A:1016125726789
Spohn M, Pötsch EM, Eichorst SA, Woebken D, Wanek W, Richter A (2016) Soil microbial carbon use efficiency and biomass turnover in a long-term fertilization experiment in a temperate grassland. Soil Biol Biochem 97:168–175. https://doi.org/10.1016/j.soilbio.2016.03.008
Tao F, Huang Y, Hungate BA, Manzoni S, Frey SD, Schmidt MWI, Reichstein M, Carvalhais N, Ciais P, Jiang L, Lehmann J, Wang YP, Houlton BZ, Ahrens B, Mishra U, Hugelius G, Hocking TD, Lu X, Shi Z, Viatkin K, Vargas R, Yigini Y, Omuto C, Malik AA, Peralta G, Cuevas-Corona R, Di Paolo LE, Luotto I, Liao C, Liang YS, Saynes VS, Huang X, Luo Y (2023) Microbial carbon use efficiency promotes global soil carbon storage. Nature 618 (7967):981–985. https://doi.org/10.1038/s41586-023-06042-3
Tian J, Pausch J, Yu G, Blagodatskaya E, Gao Y (2015) Aggregate size and their disruption affect ^{14}C-labeled glucose mineralization and priming effect. Appl Soil Ecol 90:1–10. https://doi.org/10.1016/j.apsoil.2015.01.014
Tian J, Pausch J, Yu G, Blagodatskaya E, Kuzyakov Y (2016) Aggregate size and glucose level affect priming sources: a three-source-partitioning study. Soil Biol Biochem

97:199–210. https://doi.org/10.1016/j.soilbio.2016.03.013
von Lützow M, Kögel-Knabner I, Ekschmitt K, Matzner E, Guggenberger G, Marschner B, Flessa H (2006) Stabilization of organic matter in temperate soils: mechanisms and their relevance under different soil conditions - a review. Eur J Soil Sci 57 (4):426–445. https://doi.org/10.1111/j.1365-2389.2006.00809.x
Witzgall K, Vidal A, Schubert DI, Hoeschen C, Schweizer SA, Buegger F, Pouteau V, Chenu C, Mueller CW (2021) Particulate organic matter as a functional soil component for persistent soil organic carbon. Nat Commun 12 (1):4115. https://doi.org/10.1038/s41467-021-24192-8
Zhang D, Wu B, Li J, Cheng X (2023) Soil microbial relative resource limitation exhibited contrasting seasonal patterns along an elevational gradient in Yulong Snow Mountain. Funct Ecol 37 (5):1328–1338. https://doi.org/10.1111/1365-2435.14297
Zhang Q, Li X, Liu J, Liu J, Han L, Wang X, Liu H, Xu M, Yang G, Ren C, Han X (2023) The contribution of microbial necromass carbon to soil organic carbon in soil aggregates. Appl Soil Ecol 190:104985. https://doi.org/10.1016/j.apsoil.2023.104985

Figure Legends

Fig. 1 Experimental design and initial soil resource properties in broad-leaved and coniferous forest soils. (a) Schematic of forest sampling, aggregate separation, and the C, N, and C plus N addition experiment. The two forests were sampled separately; bulk soil and three aggregate size fractions (1-2, 0.25-1, and <0.25 mm) were analyzed. C was supplied as ^{13}C-labeled glucose and N as NH_4Cl. (b) Initial soil organic carbon (SOC), total nitrogen (TN), SOC: TN ratio, dissolved organic carbon (DOC), dissolved organic nitrogen (DON), and available phosphorus (AP) across soil fractions. BF, broad-leaved forest; CF, coniferous forest. Error bars represent standard error. Capital letters indicate significant differences between the two forest soils. Lowercase letters indicate significant differences among soil aggregate fractions.

Fig. 2 Initial microbial biomass and extracellular enzyme allocation across aggregate size fractions. (a, b) Microbial biomass carbon (MBC) and nitrogen (MBN), respectively. (c) Relationship between MBC and MBN in the two forest soils. (d) Standardized activities (Z-scores) of C-acquiring α-glucosidase (AG) and β-glucosidase (BG), N-acquiring β-1,4-N-acetylglucosaminidase (NAG) and leucine aminopeptidase (LAP), and P-acquiring alkaline phosphatase (AP). (e) Relative C- and N-acquiring enzyme allocation, EC: (EC + EN), relative C- and P-acquiring enzyme allocation, EC: (EC + EP). (f) Enzyme vector length and angle by soil fraction. Error bars represent standard error. Capital letters are significant difference between the two forests. Lowercase letters are significant difference among different soil aggregate sizes. See Fig. 1 for abbreviations.

Fig. 3 Priming effect (a, b) and net carbon sequestration (c, d) in different aggregate sizes under C and N addition in broad-leaved and coniferous forest soils. Error bars represent standard error. Lowercase letters are significant difference among different soil aggregate sizes under the same treatment. Asterisks indicate statistically significant difference at $P < 0.05$ among treatments. See Fig. 1 for abbreviations.

Fig. 4 Microbial carbon use efficiency (CUE) (a, b) and microbial metabolic entropy (qCO_2) (c, d) under C and N addition in broad and coniferous forest soils. Lowercase letters are significant difference among different soil aggregate sizes under the same treatment. Asterisks indicate statistically significant difference at $P < 0.05$ among treatments. See Fig. 1 for other abbreviations.

Fig. 5 Relationships of net carbon sequestration with priming effect (a), microbial carbon

use efficiency (CUE) (b) and microbial metabolic entropy (qCO_2) (c), as well as the CUE and qCO_2 related to soil properties, microbial traits and enzyme activity in different soil aggregate sizes (d). The color represents of Spearman's rank correlation (tangerine, negative correlation; green, positive correlation). DOC, dissolved organic carbon; DON, dissolved organic nitrogen; AN, soil available nitrogen; AP, soil available phosphorus; MBC, microbial biomass carbon; MBN, microbial biomass; EC, carbon-acquisition enzyme (the sum of AG and BG); EN, nitrogen-acquisition enzyme (the sum of NAG and LAP); EP, phosphorus-acquisition enzyme (AP). $*P < 0.05$; $**P < 0.01$; $***P < 0.001$.

Fig. 6 Partial least squares path modelling (PLS-PM) (a-d) evaluated major pathways of soil properties, microbial parameters and enzyme activity on CUE, qCO_2, PE and NCS of different soil aggregate size. Red arrows indicate positive association, blue arrows indicate negative association and grey arrows indicate no significant association. See Fig. 1 and Fig. 5 for abbreviations.

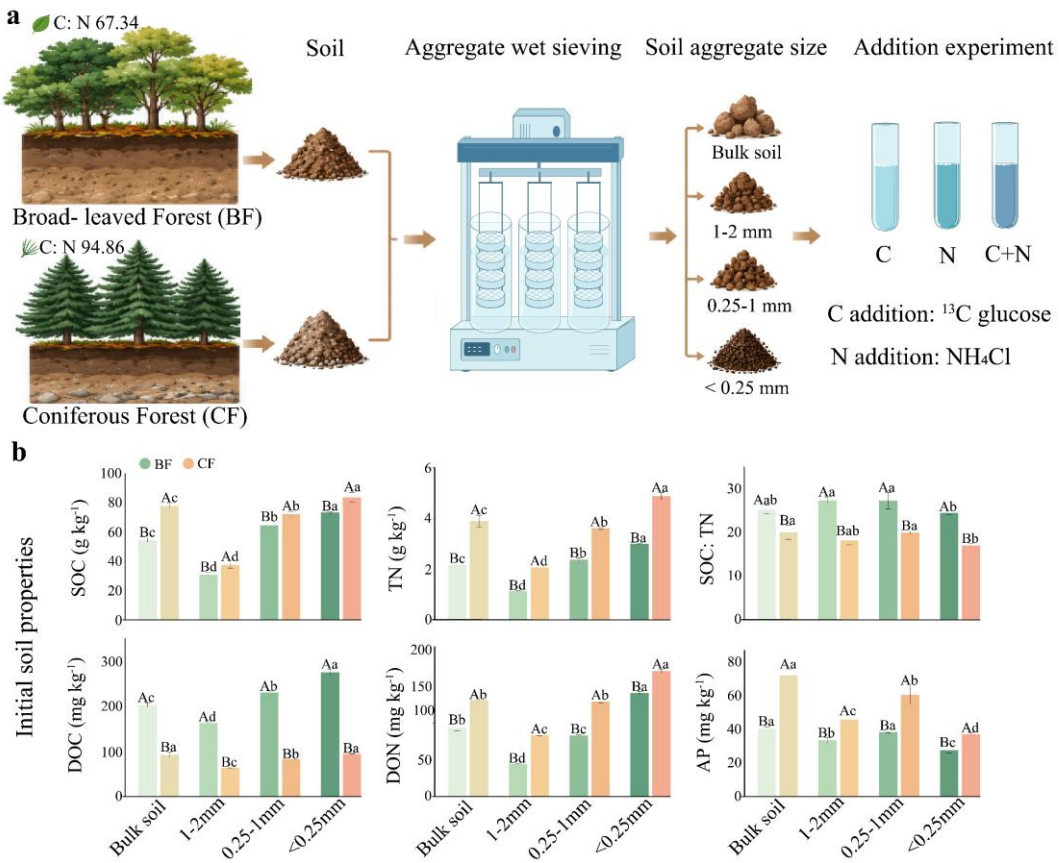

a
C: N 67.34
Broad- leaved Forest (BF)
C: N 94.86
Coniferous Forest (CF)
Soil
Aggregate wet sieving
Soil aggregate size
Addition experiment
Bulk soil
1-2 mm
0.25-1 mm
< 0.25 mm
C
N
C+N
C addition: 13C glucose
N addition: NH4Cl
b
BF
CF
Initial soil properties
SOC (g kg-1)
TN (g kg-1)
SOC: TN
DOC (mg kg-1)
DON (mg kg-1)
AP (mg kg-1)
Bulk soil
1-2mm
0.25-1mm
<0.25mm

Fig. 1

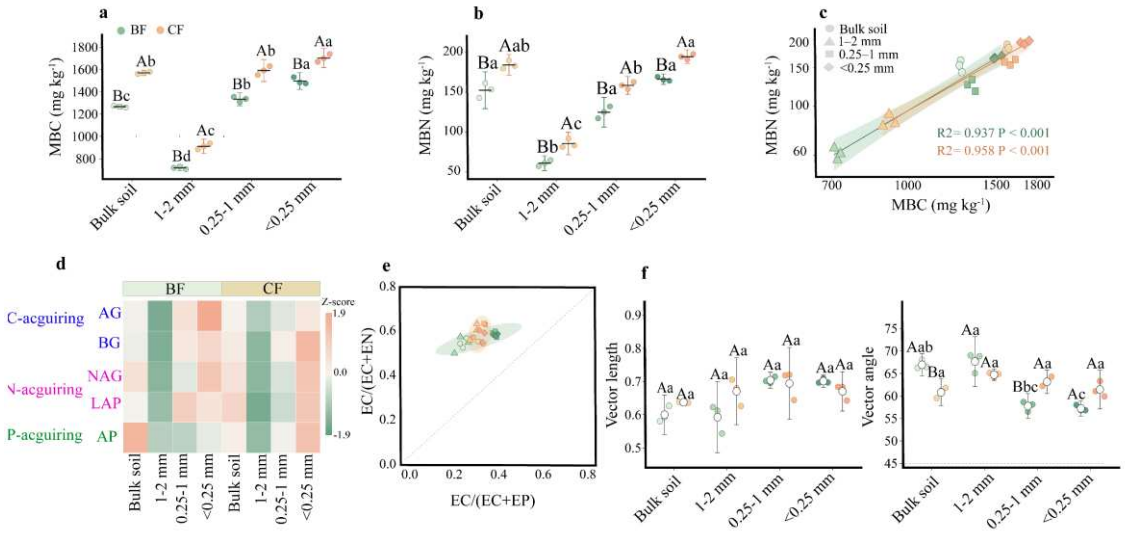
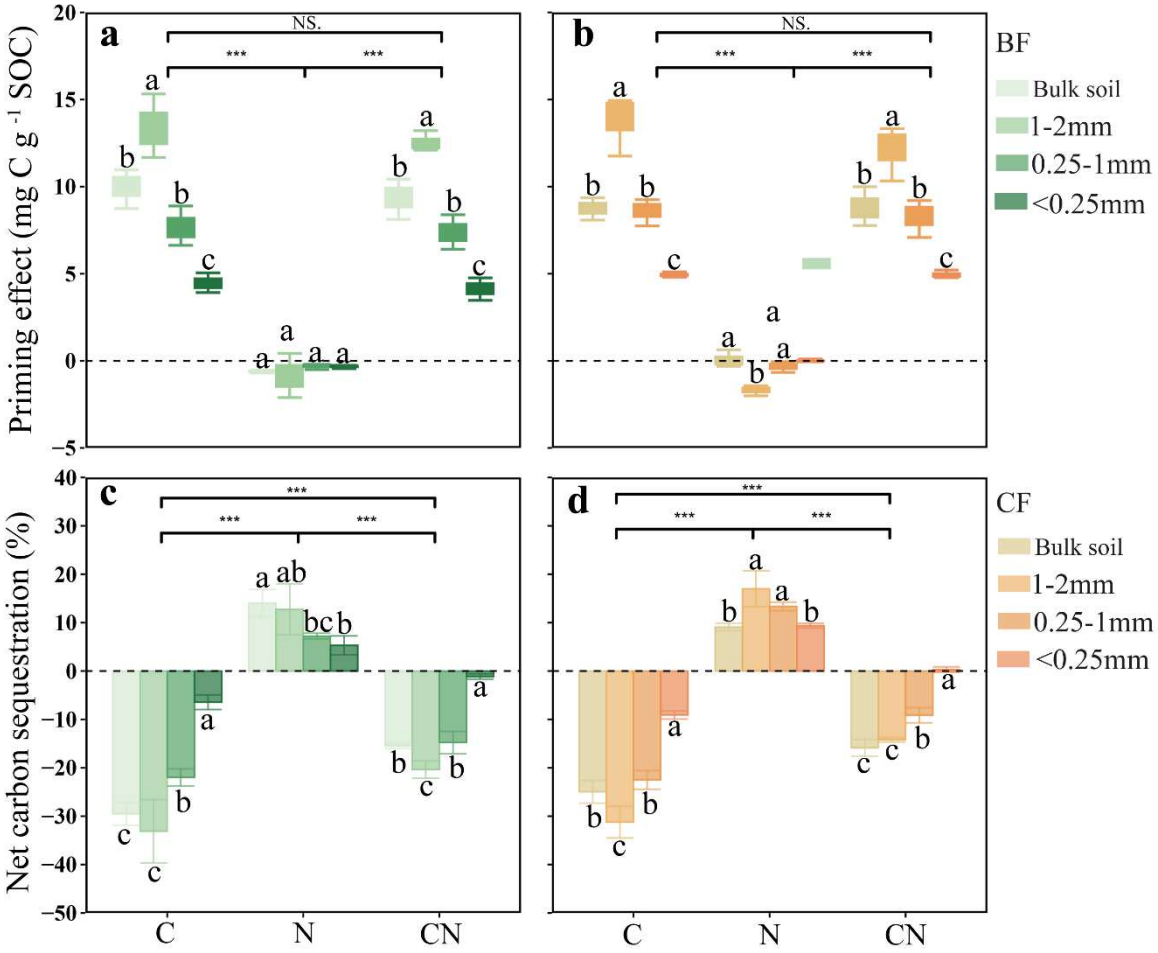

a
BF
CF
MBC (mg kg⁻¹)
Bulk soil
1-2 mm
0.25-1 mm
<0.25 mm
b
MBN (mg kg⁻¹)
c
Bulk soil
1–2 mm
0.25–1 mm
<0.25 mm
R2= 0.937 P < 0.001
R2= 0.958 P < 0.001
MBC (mg kg⁻¹)
MBN (mg kg⁻¹)
d
BF
CF
Z-score
C-acguiring
AG
BG
N-acguiring
NAG
LAP
P-acguiring
AP
e
EC/(EC+EN)
EC/(EC+EP)
f
Vector length
Vector angle

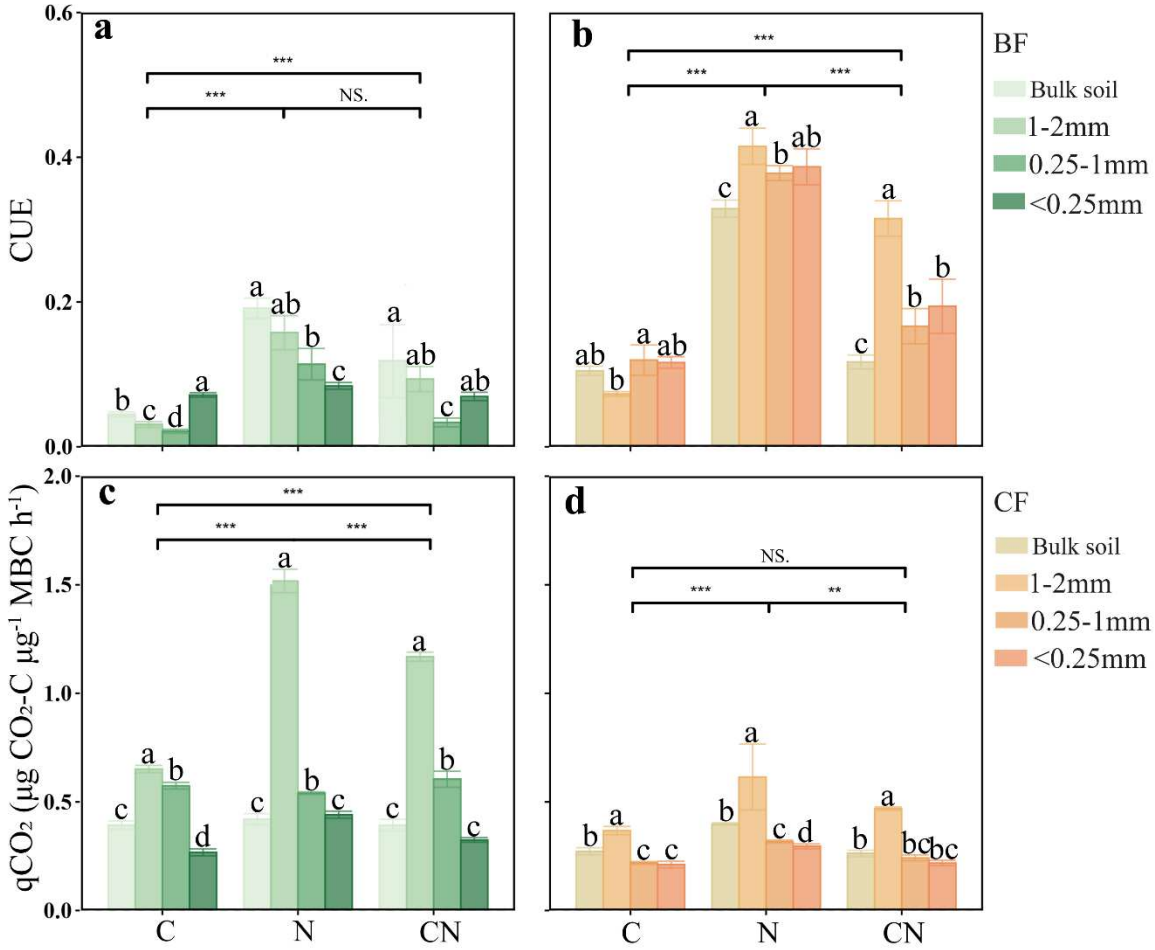
Fig. 2



705

706 **Fig. 3**

707



708

709 **Fig. 4**

710

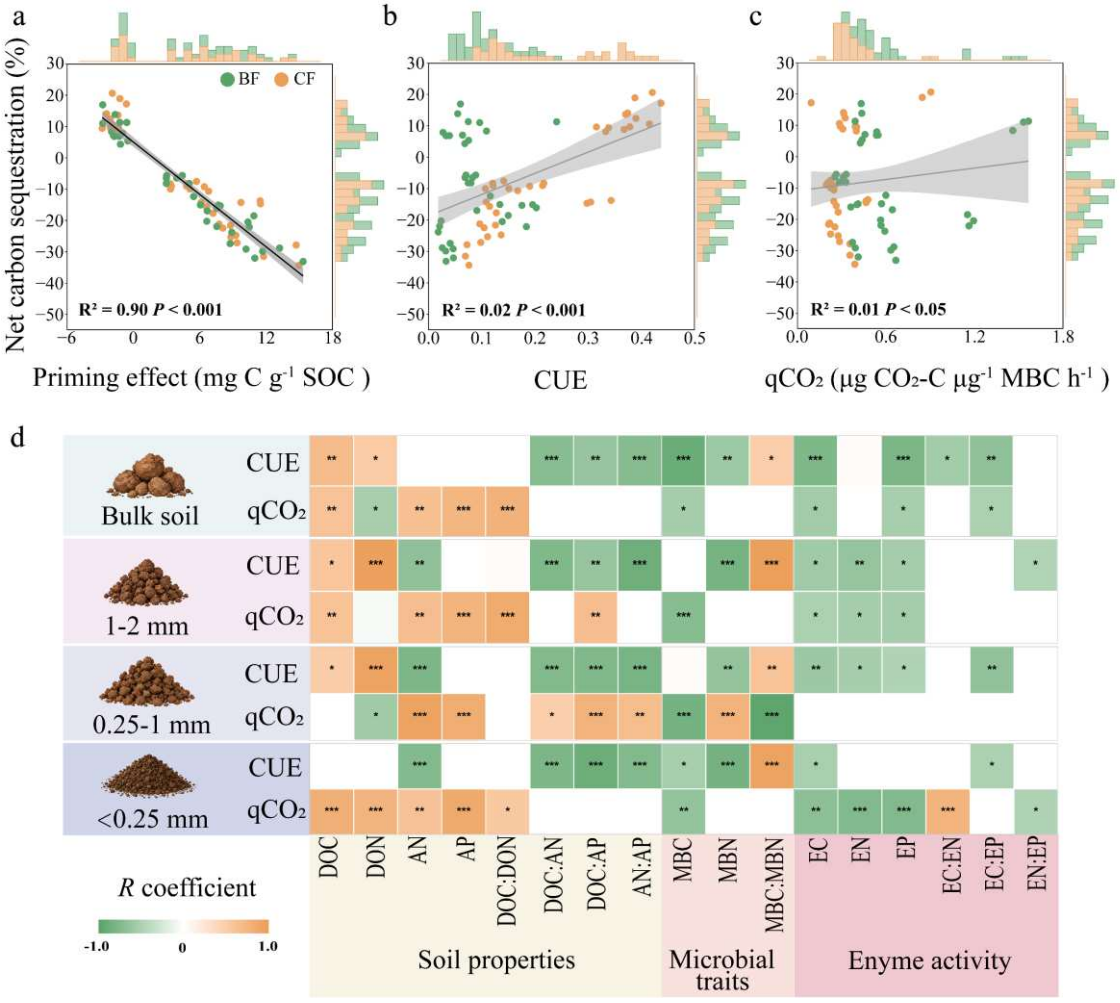

a
b
c
d
Net carbon sequestration (%)
BF
CF
R² = 0.90 P < 0.001
R² = 0.02 P < 0.001
R² = 0.01 P < 0.05
Priming effect (mg C g-1 SOC)
CUE
qCO2 (μg CO2-C μg-1 MBC h-1)
Bulk soil
1-2 mm
0.25-1 mm
<0.25 mm
CUE
qCO2
R coefficient
-1.0
0
1.0
DOC
DON
AN
AP
DOC:DON
DOC:AN
DOC:AP
AN:AP
MBC
MBN
MBC:MBN
EC
EN
EP
EC:EN
EC:EP
EN:EP
Soil properties
Microbial traits
Enyme activity

Fig. 5

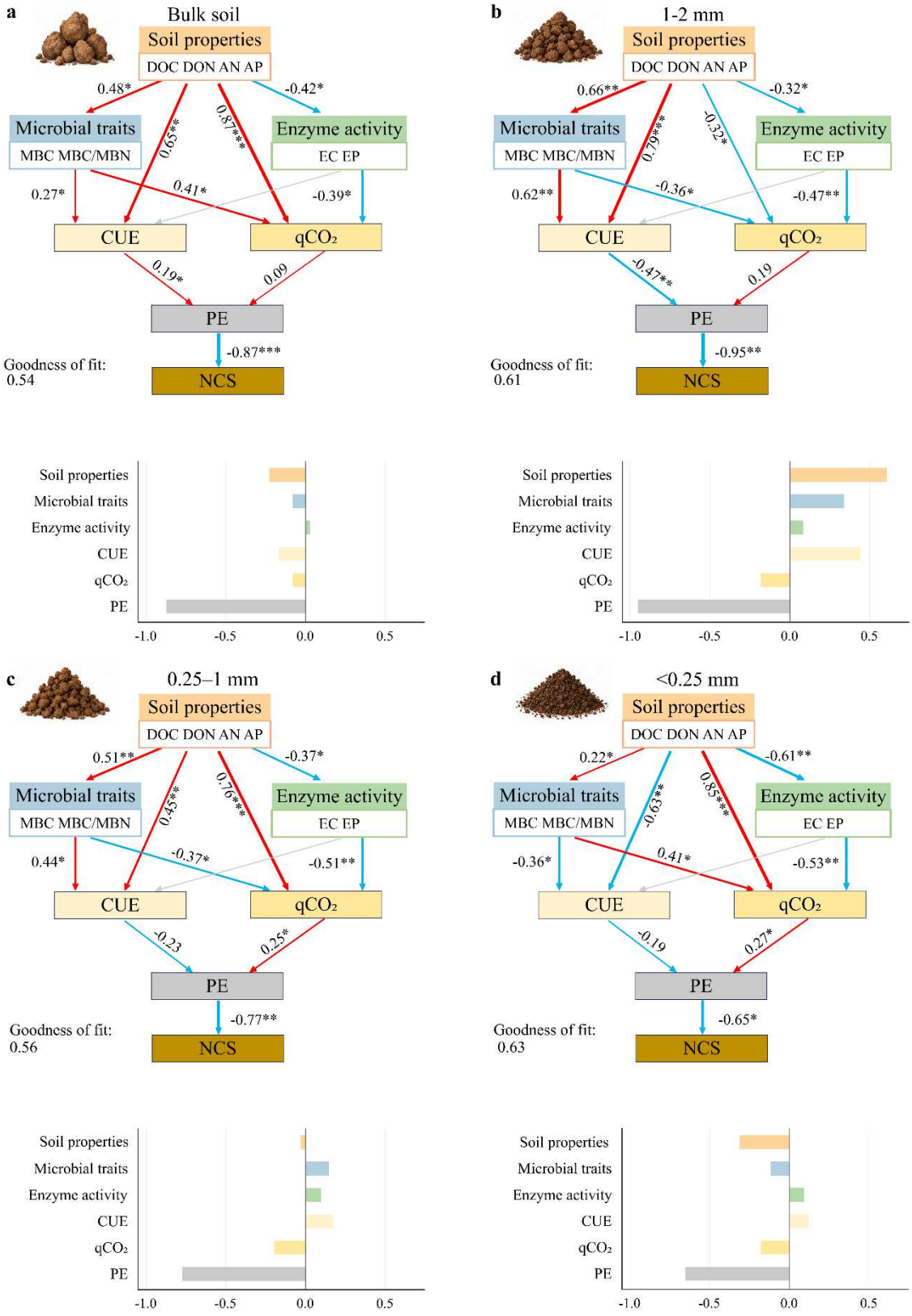

a
Bulk soil
Soil properties
DOC DON AN AP
Microbial traits
MBC MBC/MBN
Enzyme activity
EC EP
CUE
qCO2
PE
NCS
0.48*
-0.42*
0.65**
0.87***
0.27*
0.41*
-0.39*
0.19*
0.09
-0.87***
Goodness of fit:
0.54
b
1-2 mm
Soil properties
DOC DON AN AP
Microbial traits
MBC MBC/MBN
Enzyme activity
EC EP
CUE
qCO2
PE
NCS
0.66**
-0.32*
0.79***
-0.32*
0.62**
-0.36*
-0.47**
-0.47**
0.19
-0.95**
Goodness of fit:
0.61
Soil properties
Microbial traits
Enzyme activity
CUE
qCO2
PE
-1.0
-0.5
0.0
0.5
Soil properties
Microbial traits
Enzyme activity
CUE
qCO2
PE
-1.0
-0.5
0.0
0.5
c
0.25–1 mm
Soil properties
DOC DON AN AP
Microbial traits
MBC MBC/MBN
Enzyme activity
EC EP
CUE
qCO2
PE
NCS
0.51**
-0.37*
0.45**
0.76***
0.44*
-0.37*
-0.51**
-0.23
0.25*
-0.77**
Goodness of fit:
0.56
d
<0.25 mm
Soil properties
DOC DON AN AP
Microbial traits
MBC MBC/MBN
Enzyme activity
EC EP
CUE
qCO2
PE
NCS
0.22*
-0.61**
-0.63**
0.85***
-0.36*
0.41*
-0.53**
-0.19
0.27*
-0.65*
Goodness of fit:
0.63
Soil properties
Microbial traits
Enzyme activity
CUE
qCO2
PE
-1.0
-0.5
0.0
0.5
Soil properties
Microbial traits
Enzyme activity
CUE
qCO2
PE
-1.0
-0.5
0.0
0.5

Fig. 6

Supplementary Files

This is a list of supplementary files associated with this preprint. Click to download.

- SupplementaryInformation.docx